https://doi.org/10.2352/EI.2023.35.9.IPAS-290


# Deploying Machine Learning Based Segmentation for Scientific Imaging Analysis at Synchrotron Facilities

***Guanhua Hao***[†,1]***, Eric J. Roberts***[†,2,3]***, Tanny Chavez***[1]***, Zhuowen Zhao***[1]***, Elizabeth A. Holman***[1]***, Howard Yanxon***[4]***, Adam Green***[1]***, Harinarayan Krishnan***[1,2]***, Daniela Ushizima***[2,5]***, Dylan McReynolds***[1]***, Nicholas Schwarz***[4]***, Petrus H. Zwart***[*,2,3]***, Alexander Hexemer***[1]***, and Dilworth Y. Parkinson***[**,1]

[1] ***Advanced Light Source (ALS), Lawrence Berkeley National Laboratory; Berkeley, CA 94720***
[2] ***Center for Advanced Mathematics for Energy Research Applications (CAMERA), Lawrence Berkeley National Laboratory; Berkeley, CA 94720***
[3] ***Molecular Biophysics and Integrated Bioimaging (MBIB), Lawrence Berkeley National Laboratory; Berkeley, CA 94720***
[4] ***Advanced Photon Source (APS), Argonne National Laboratory; Lemont, IL 60439***
[5] ***Computational Research Division (CRD), Lawrence Berkeley National Laboratory; Berkeley, CA 94720***
[†] ***Authors contributed equally***
[*] ***Corresponding author 1: phzwart@lbl.gov***
[**] ***Corresponding author 2: dyparkinson@lbl.gov***

## Abstract

*Scientific user facilities present a unique set of challenges for image processing due to the large volume of data generated from experiments and simulations. Furthermore, developing and implementing algorithms for real-time processing and analysis while correcting for any artifacts or distortions in images remains a complex task, given the computational requirements of the processing algorithms. In a collaborative effort across multiple Department of Energy national laboratories, the "MLExchange" project is focused on addressing these challenges. MLExchange is a Machine Learning framework deploying interactive web interfaces to enhance and accelerate data analysis. The platform allows users to easily upload, visualize, label, and train networks. The resulting models can be deployed on real data while both results and models could be shared with the scientists. The MLExchange web-based application for image segmentation allows for training, testing, and evaluating multiple machine learning models on hand-labeled tomography data. This environment provides users with an intuitive interface for segmenting images using a variety of machine learning algorithms and deep-learning neural networks. Additionally, these tools have the potential to overcome limitations in traditional image segmentation techniques, particularly for complex and low-contrast images.*

## Introduction

The scientific community relies on scientific instrumentation at light and neutron source user facilities to perform science that is impossible anywhere else. Beamlines are significant producers of scientific data, and image-based data constitutes a significant part of this, with many instruments producing terabytes of image data per day. Beyond the challenges of moving and storing data at high rates and volumes is the challenge of developing and implementing algorithms for processing and analyzing data in real-time to produce immediate results while accurately correcting for artifacts. Thus, there is a pressing need for coordinated tools that can build reproducible pipelines for optimizing the user experience and experiment efficiency.

Recent advances in scientific machine learning (ML) have proven to be a powerful tool to enhance data analysis – especially image processing. Scientific imaging analysis faces unique hurdles as it often requires domain expertise to decode intrinsic relationships between image features. Applying a ML-based pipeline in this context thus requires flexibility and adaptability to many different specific use cases [1]. Moreover, to allow access for all beamline users, many of whom have no experience with ML or high performance image processing, the solution has to be easy-to-use and must allow scaling to the size of data produced at modern synchrotron instruments.

As a collaborative effort across several Department of Energy (DOE) national laboratories, we have developed a platform called "MLExchange" to provide easily-accessible interfaces for ML-infused tools. This Machine Learning Operations (MLOps) platform features multiple interactive web interfaces allowing for easy exchange, visualization, and labeling of datasets, as well as training and testing of various ML models and techniques. The platform is designed to be expandable and collaborative, to enable users to contribute new algorithms and customize existing algorithms for their specific scientific needs [2].

One of the web-based applications within the platform focuses on image segmentation tasks. This application provides an intuitive interface for users to segment images using ML algorithms, such as deep learning neural networks. Traditional segmentation techniques such as thresholding or watershedding [3] can struggle with complex or low contrast images. ML, on the other hand, has the potential to identify features and effectively segment such images [4, 5, 6] despite obstacles such as noise and artifacts sometimes present in tomography data sets.

Below is an introduction to the web-based segmentation interface within MLExchange.

## A Web-based Segmentation Interface

The MLExchange Segmentation Application has been deployed on a centralized server at the Advanced Light Source, Lawrence Berkeley National Laboratory. It consists of five primary components: a File Manager tab, an Image Display session, an Annotation Panel, a Model Selection Panel, and a Table of Jobs (as depicted in Figure 1). To initiate a segmentation task, users upload an image stack through the drag-and-drop box, which is then displayed in the Image Display section, equipped with a slice navigation bar.

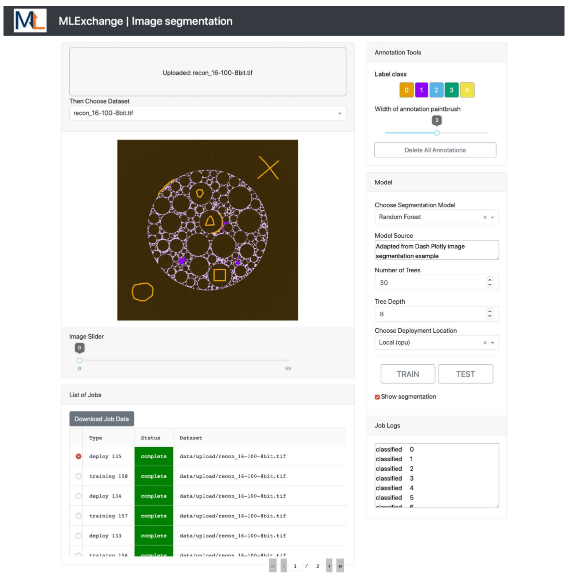


*Figure 1. Layout of the MLExchange image segmentation application, with a demonstration of ML guided segmentation for X-ray microCT images. The manually labeled sparse annotations are colored purple and orange as the ground truth for training, while model predictions are colored light yellow and violet as the background and sample, respectively.*

In the Model Selection Panel, users then can choose from three currently available algorithms: a Supervised Random Forest Classifier, an Unsupervised K-Means Clustering Algorithm, or a Supervised Mixed-Scale Dense Convolutional Neural Network (MSDNet). Upon selection, the default model parameters are automatically set, which can be adjusted if necessary. Various training parameter choices may also be selected here, including the number of epochs, loss criterion, learning rate, and the optimizer. If a supervised model is selected, ground truth information must be provided using the Annotation Panel, where regions of interest can be color-coded to represent different classes.

As in other ML workflows, the model will undergo a train-test process. The MLExchange Segmentation Application training session is initiated by hitting the TRAIN button, and progress can be monitored in the Table of Jobs at the bottom of the application. Upon completion, pressing the TEST button triggers the segmentation process, analyzing the entire image stack with the trained model. The segmentation result can be displayed by toggling on the “Show Segmentation” option, which color-codes each pixel according to its corresponding class. Completed requests can be retrieved and revisited in the Table of Jobs section for future needs.

## Mixed-Scale Dense Convolutional Neural Network

One deep learning network model has been integrated into the segmentation application. The mixed-scale dense network (MSDNet) [7] was developed as a deep learning framework for image classification and pixel-by-pixel segmentation tasks with a relatively simple architecture containing roughly two to three orders of magnitude *fewer* trainable parameters than U-Nets [8] and other typical encoder-decoder convolutional neural networks [9, 10]. MSDNets have proven effective and been tested in several use cases for tomographic reconstruction [11, 12, 13, 14], nano-CT denoising [15], segmentation of sub-nuclear structures in focused-ion beam scanning electron microscopy (FIB-SEM) [16], X-ray scattering imaging inpainting [17], and X-ray in-line phase contrast imaging [18].

Benefits of MSDNet can be attributed to two distinct details in its architecture. First, MSDNet replaces typical upscaling and downscaling operations (such as transposed convolutions and maximum pooling) with dilated convolutions [19, 20]. Convolutions with integer dilations operate in the same manner as standard convolutions, but by inflating the kernel with gaps between entries that expand the kernel’s receptive field; e.g. a $3 \times 3$ dilated convolution with a dilation of 5 has a receptive field of $11 \times 11$ pixels, as vertically- and horizontally-adjacent entries in the kernel are spaced 5 pixels apart. Second, image features from different length scales are mixed together by densely connecting *all* network layers with dilated convolutions and summing the results at each layer, as depicted in the 3-layer MSDNet diagram in Figure 2. Dense and direct connections in this manner is only feasible with dilated convolutions since they preserve spatial dimensionality, allowing *all* previous layers’ outputs to be used as input in computing the next layer’s feature map, effectively creating a network full of skip connections [21] of all possible lengths. This allows MSDNets to train on lower amounts of data than what is required of other deep learning networks, as the dense interconnectivity yields maximum reusability of *all* input and intermediate information. Furthermore, dense connections assist in the recovery of lost spatial information [22] and help alleviate the vanishing gradient problem [23], which, when combined with a relatively small number of trainable parameters, allows for faster model convergence that remains robust to overfitting.

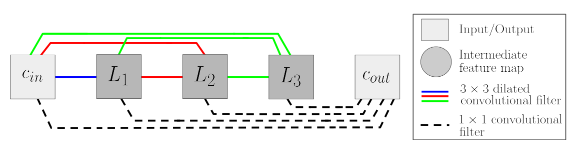


*Figure 2. Schematic of a 3-layer mixed-scale dense network (MSDNet). Blue, green, and red solid lines represent $3 \times 3$ dilated convolutions between each possible pairing of the input and hidden layers $L_i$, with different dilations assigned to each color. Black dotted lines represent $1 \times 1$ convolutional operators connecting all hidden layers and the input to the final output, effectively resulting in a linear sum with learned weights between all previous layers.*

User-defined custom implementations of MSDNets were accomplished through the Python-based deep learning software library *dlsia* (**D**eep **L**earning for **S**cientific **I**mage **A**nalysis), which allows one to easily tune the network hyperparameters and interlayer operations to optimize its performance. Further *dlsia* documentation may be found at `https://dlsia.readthedocs.io/en/latest/`.

### ML-aided Tomography Segmentation

To evaluate the performance of the MLExchange segmentation application, a study was conducted using synthetic tomography images from the TomoBank phantom foam data set [24], pictured in Figure 3. In this series of data sets, one high-quality (HQ) and five problematic versions of the raw data are synthesized, with problems mimicking limitations often seen in real tomography scans such as only using a limited number of angles, noise, and limited angular range. For the purposes of demonstrating MLExchange and the segmentation interface, we did not use advanced reconstruction approaches - rather we used a consistent set of parameters to reconstruct each data set using the ASTRA Toolbox [25, 26]. We reconstructed a 100-slice sample of each data set for this demonstration.

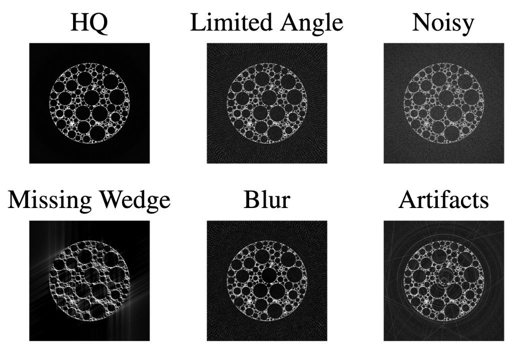


***Figure 3.*** *An overview of the reconstructed phantom foam data set, with HQ picturing the high quality reconstructed slices. Other images represent various degrees of limitations encountered in tomography scans.*

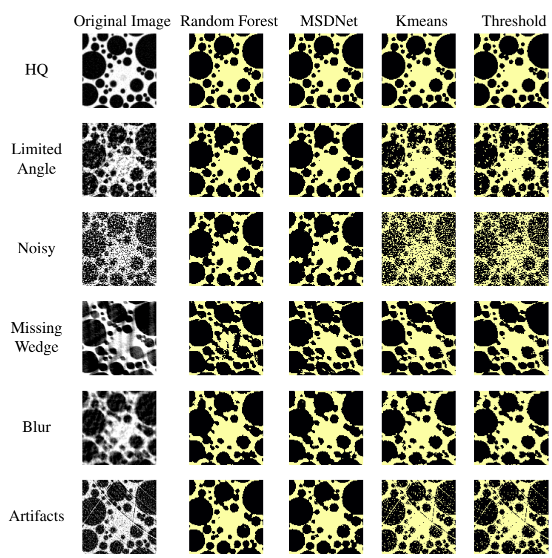


***Figure 4.*** *Visualization of the segmentation results for a zoomed-in region of the sample. Each row corresponds to the data set described in Figure 3. The phantom foam is marked in yellow, while the background is marked in black.*

Three types of ML-based segmentation were performed: a Supervised Random Forest Classifier with 30 decision trees and a tree depth of 8; a Supervised Mixed-Scale Dense Convolutional Neural Network with 12 convolutional layers, max dilation of 6 and a learning rate of 0.01 for 50 epochs, optimized using the ADAM algorithm [27] to update the model weights by minimizing the cross entropy loss criterion; and an Unsupervised K-means Clustering algorithm with 2 clusters and a maximum iteration of 300. For both supervised models, training data consisted of *only* a pair of single images: the first image in each of the 100-slice samples and a corresponding mask with sparsely annotated labeling as a target. In this single mask, used across all 6 data sets to ensure consistency, roughly 16% of pixels were labeled, of which the foreground-to-background ratio was roughly 1:40. For the unsupervised method, only the first image is used in model training. Lastly, a traditional threshold-based segmentation [28] was performed as a baseline comparison, with all sets sharing the same threshold value.

The segmented results are presented in Figure 4 with a zoomed in portion of the sample to show details. The performance of each individual model was evaluated using the F1 score [29], defined as the harmonic mean of model precision and recall, and the Intersection Over Union (IoU) metric, also known as the Jaccard index, which measures the ratio of correct class predictions over the combined ground truth and predictions for said class. The mean F1 and IoU of each stack are presented in Figures 5 and 6, respectively.

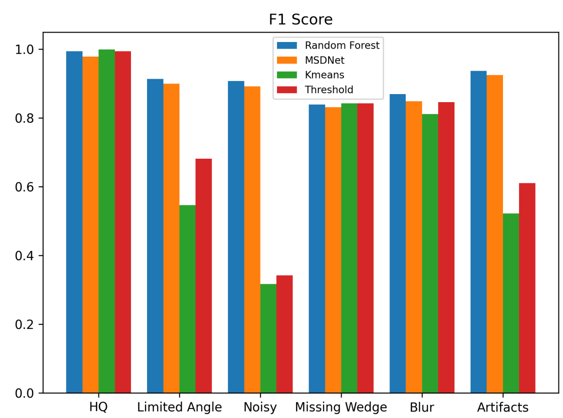


***Figure 5.*** *F1 score of the segmentation result. Each color represents one segmentation method (Random Forest, MSDNet, K-means and traditional Thresholding), and the bar value is calculated from the mean over the 100 segmented images for each technique.*

The results of the segmentation study on synthetic tomography images indicate the robustness of the two supervised learning methods, the Random Forest classifier and the MSDNet, in handling noise and artifacts. Despite being trained on limited ground truth information, the Random Forest classifier showed a mean F1 score centered around 0.91 and a mean Intersection Over Union (IoU) score centered around 0.84, while the MSDNet mean F1 score of 0.90 and a mean IoU score of 0.81. In contrast, both the unsupervised K-Means Clustering method and the traditional thresholding technique demonstrated strong performance with high-quality data, yielding mean F1 and IoU scores approaching 1. However, the performance of these methods drastically reduced with the introduction of noise, indicating their sen-

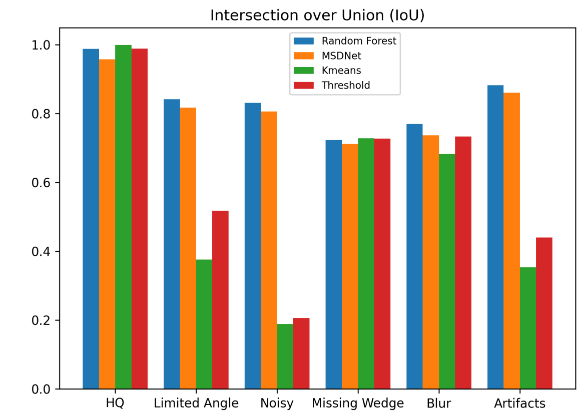


***Figure 6.*** *Intersection Over Union (IoU) of the segmentation result. Each color represents one segmentation method (Random Forest, MSDNet, K-means and traditional Thresholding), and the bar value is calculated from the mean over the 100 segmented images for each technique.*

sitivity to image quality and contrast. It is worth noting that the quality of both the neural network classifier and the Random Forest method are dependent on both how much of the image is annotated, and also where and how. This is especially true for the MSDNet; Deep learning neural network models typically require vast amounts of training data [30], though the MSDNet overcame this via the dense interconnectivity between layers that allows for maximum reusability for the sparsely annotated single image training data set. Fortunately, the interactive nature of the MLExchange user interface allows one to rapidly iterate between annotation paradigms - sparse or dense - to enhance the performance for a particular data set under any classification scheme.

## Summary and Looking Forward

The MLExchange platform is an MLOps platform that provides web-based interfaces for the training and testing of ML models, specifically designed to address the challenges in scientific data processing. The MLExchange Segmentation Application, a key component of the platform, enables users to segment images generated from scientific experiments using ML algorithms, including deep learning neural networks, and has been evaluated using synthetic tomography images from the TomoBank phantom foam dataset, showing improved results compared to traditional threshold-based segmentation techniques. So far, several other test cases have been successfully deployed in the segmentation application, including a number of different X-ray microCT dataset and one X-ray scattering dataset. Particularly impressive in the MLExchange supervised learning schemes is the ability to accommodate sparse or incomplete labeling of ground truth data, as evidenced by the sparse manual labeling of classes.

The MLExchange platform serves as a central repository containing a collection of community-sourced algorithms, models, and data sets. Users can access and utilize these contributions to analyze and annotate their experimental data, providing new insights and refinements to the shared repository. This platform offers facility users an accessible and convenient solution to their image processing needs. The user-friendly interface enables the selection, download, and implementation of ML solutions for testing on their own experimental data. The platform operates as a web-based system, with all applications and pipelines contained in a centralized deployment, requiring only a web browser login for access and eliminating the need for any local installations.

## Acknowledgement

This work was performed and partially supported by the US Department of Energy (DOE), Office of Science, Office of Basic Energy Sciences Data, Artificial Intelligence and Machine Learning at the DOE Scientific User Facilities program under the MLExchange Project (award No. 107514). This research used resources of the Advanced Light Source, which is a DOE Office of Science User Facility under contract No. DE-AC02-05CH11231. This work was partly funded through the Center for Advanced Mathematics for Energy Research Applications (CAMERA), which is jointly funded by the Advanced Scientific Computing Research (ASCR) and Basic Energy Sciences (BES) within the Department of Energy's Office of Science, as well as by the Laboratory Directed Research and Development Program of Lawrence Berkeley National Laboratory, under US Department of Energy contract no. DE-AC02-05CH11231. Further support originates from the National Institute of General Medical Sciences of the National Institutes of Health (NIH) under Award 5R21GM129649-02.

## References

[1] Howard Yanxon, James Weng, Hannah Parraga, Wenqian Xu, Uta Ruett, and Nicholas Schwarz. Artifact identification in X-ray diffraction data using machine learning methods. *Journal of Synchrotron Radiation*, 30(1):137–146, Jan 2023.

[2] Zhuowen Zhao, Tanny Chavez, Elizabeth A. Holman, Guanhua Hao, Adam Green, Harinarayan Krishnan, Dylan McReynolds, Ronald J. Pandolfi, Eric J. Roberts, Petrus H. Zwart, Howard Yanxon, Nicholas Schwarz, Subramanian Sankaranarayanan, Sergei V. Kalinin, Apurva Mehta, Stuart I. Campbell, and Alexander Hexemer. Mlexchange: A web-based platform enabling exchangeable machine learning workflows for scientific studies. In *2022 4th Annual Workshop on Extreme-scale Experiment-in-the-Loop Computing (XLOOP)*, pages 10–15, 2022.

[3] Luc Vincent and Pierre Soille. Watersheds in digital spaces: an efficient algorithm based on immersion simulations. *IEEE Transactions on Pattern Analysis & Machine Intelligence*, 13(06):583–598, 1991.

[4] Alexandre Fioravante de Siqueira, Daniela M Ushizima, and Stéfan J van der Walt. A reusable neural network pipeline for unidirectional fiber segmentation. *Scientific data*, 9(1):32, 2022.

[5] Yuriy Sinchuk, Pierre Kibleur, Jan Aelterman, Matthieu N Boone, and Wim Van Paepegem. Variational and deep learning segmentation of very-low-contrast x-ray computed tomography images of carbon/epoxy woven composites. *Materials*, 13(4):936, 2020.

[6] Emmanuel Moebel, Antonio Martinez-Sanchez, Lorenz Lamm, Ricardo D Righetto, Wojciech Wietrzynski, Sahradha Albert, Damien Larivière, Eric Fourmentin, Stefan Pfeffer, Julio Ortiz, et al. Deep learning improves macromolecule identification in 3d cellular cryo-electron tomograms. *Nature methods*, 18(11):1386–1394, 2021.

[7] Daniël M Pelt and James A Sethian. A mixed-scale dense convolutional neural network for image analysis. *Proceedings of the National Academy of Sciences*, 115(2):254–259, 2018.

[8] Olaf Ronneberger, Philipp Fischer, and Thomas Brox. U-net: Convolutional networks for biomedical image segmentation. In *Inter-*

*national Conference on Medical image computing and computer-assisted intervention*, pages 234–241. Springer, 2015.

[9] David E Rumelhart, Geoffrey E Hinton, and Ronald J Williams. Learning internal representations by error propagation. Technical report, California Univ San Diego La Jolla Inst for Cognitive Science, 1985.

[10] Yann LeCun, Léon Bottou, Yoshua Bengio, and Patrick Haffner. Gradient-based learning applied to document recognition. *Proceedings of the IEEE*, 86(11):2278–2324, 1998.

[11] Daniël M Pelt, Kees Joost Batenburg, and James A Sethian. Improving tomographic reconstruction from limited data using mixed-scale dense convolutional neural networks. *Journal of Imaging*, 4(11):128, 2018.

[12] Jordi Minnema, Maureen van Eijnatten, Allard A Hendriksen, Niels Liberton, Daniël M Pelt, Kees Joost Batenburg, Tymour Forouzanfar, and Jan Wolff. Segmentation of dental cone-beam ct scans affected by metal artifacts using a mixed-scale dense convolutional neural network. *Medical physics*, 46(11):5027–5035, 2019.

[13] Li-av Segev-Zarko, Peter D Dahlberg, Stella Y Sun, Daniël M Pelt, Chi Yong Kim, Elizabeth S Egan, James A Sethian, Wah Chiu, and John C Boothroyd. Cryo-electron tomography with mixed-scale dense neural networks reveals key steps in deployment of toxoplasma invasion machinery. *PNAS nexus*, 1(4):pgac183, 2022.

[14] Michael Sieverts, Yoshihiro Obata, James L Rosenberg, William Woolley, Dilworth Y Parkinson, Harold S Barnard, Daniël M Pelt, and Claire Acevedo. Unraveling the effect of collagen damage on bone fracture using in situ synchrotron microtomography with deep learning. *Communications Materials*, 3(1):78, 2022.

[15] Silja Flenner, Stefan Bruns, Elena Longo, Andrew J Parnell, Kilian E Stockhausen, Martin Müller, and Imke Greving. Machine learning denoising of high-resolution x-ray nanotomography data. *Journal of Synchrotron Radiation*, 29(1):230–238, 2022.

[16] Niraj Gupta, Eric J Roberts, Song Pang, C Shan Xu, Harald F Hess, Fan Wu, Abby Dernburg, Danielle Jorgens, Petrus H Zwart, and Vignesh Kasinath. Deep learning-based identification of sub-nuclear structures in fib-sem images. *arXiv preprint arXiv:2207.09598*, 2022.

[17] Tanny Chavez, Eric J Roberts, Petrus H Zwart, and Alexander Hexemer. A comparison of deep-learning-based inpainting techniques for experimental x-ray scattering. *Journal of applied crystallography*, 55(5), 2022.

[18] Kannara Mom, Bruno Sixou, and Max Langer. Mixed scale dense convolutional networks for x-ray phase contrast imaging. *Applied optics*, 61(10):2497–2505, 2022.

[19] Fisher Yu and Vladlen Koltun. Multi-scale context aggregation by dilated convolutions. *arXiv preprint arXiv:1511.07122*, 2015.

[20] Yuhong Li, Xiaofan Zhang, and Deming Chen. Csrnet: Dilated convolutional neural networks for understanding the highly congested scenes. In *Proceedings of the IEEE conference on computer vision and pattern recognition*, pages 1091–1100, 2018.

[21] Michal Drozdzal, Eugene Vorontsov, Gabriel Chartrand, Samuel Kadoury, and Chris Pal. The importance of skip connections in biomedical image segmentation. In *Deep learning and data labeling for medical applications*, pages 179–187. Springer, 2016.

[22] Gao Huang, Zhuang Liu, Geoff Pleiss, Laurens Van Der Maaten, and Kilian Q Weinberger. Convolutional networks with dense connectivity. *IEEE transactions on pattern analysis and machine intelligence*, 44(12):8704–8716, 2019.

[23] Sergey Ioffe and Christian Szegedy. Batch normalization: Accelerating deep network training by reducing internal covariate shift. In *International conference on machine learning*, pages 448–456. PMLR, 2015.

[24] Francesco De Carlo, Doğa Gürsoy, Daniel J Ching, K Joost Batenburg, Wolfgang Ludwig, Lucia Mancini, Federica Marone, Rajmund Mokso, Daniël M Pelt, Jan Sijbers, and Mark Rivers. Tomobank: a tomographic data repository for computational x-ray science. *Measurement Science and Technology*, 29(3):034004, feb 2018.

[25] Wim van Aarle, Willem Jan Palenstijn, Jeroen Cant, Eline Janssens, Folkert Bleichrodt, Andrei Dabravolski, Jan De Beenhouwer, K. Joost Batenburg, and Jan Sijbers. Fast and flexible x-ray tomography using the astra toolbox. *Opt. Express*, 24(22):25129–25147, Oct 2016.

[26] Wim van Aarle, Willem Jan Palenstijn, Jan De Beenhouwer, Thomas Altantzis, Sara Bals, K. Joost Batenburg, and Jan Sijbers. The astra toolbox: A platform for advanced algorithm development in electron tomography. *Ultramicroscopy*, 157:35–47, 2015.

[27] Diederik P Kingma and Jimmy Ba. Adam: A method for stochastic optimization. *arXiv preprint arXiv:1412.6980*, 2014.

[28] Azriel Rosenfeld. Picture processing by computer. *ACM Computing Surveys (CSUR)*, 1(3):147–176, 1969.

[29] Nancy Chinchor and Beth M Sundheim. Muc-5 evaluation metrics. In *Fifth Message Understanding Conference (MUC-5): Proceedings of a Conference Held in Baltimore, Maryland, August 25-27, 1993*, 1993.

[30] Ian Goodfellow, Yoshua Bengio, and Aaron Courville. *Deep learning*. MIT press, 2016.

## Author Biography

*Guanhua (Tibbers) Hao received his PhD in Physics from University of Nebraska-Lincoln (2021). Since then he has worked at Advanced Light Source, Lawrence Berkeley National Laboratory, CA. He constructs algorithms and machine learning pipelines to help with analysis of image data generated by synchrotron facilities, and develops solutions to segment scientific images (microCT, GISAXS) using machine learning methods. He also works on deep learning infused image retrieval pipelines to aid for image similarity detection.*